

Effective Data Pruning through Score Extrapolation

Sebastian Schmidt^{1,3,†} Prasanga Dhungel^{1,†} Christoffer Löffler⁴ Björn Nieth⁶
 Stephan Günnemann^{1,2,5} Leo Schwinn^{1,2}

¹ Technical University of Munich, School of Computation, Information and Technology

² Munich Data Science Institute ³ BMW Group

⁴ Pontificia Universidad Católica de Valparaíso ⁵ Pruna AI

⁶ Friedrich-Alexander Universität Erlangen-Nürnberg

Abstract

Training advanced machine learning models demands massive datasets, resulting in prohibitive computational costs. To address this challenge, data pruning techniques identify and remove redundant training samples while preserving model performance. Yet, existing pruning techniques predominantly require a full initial training pass to identify removable samples, negating any efficiency benefits for single training runs. To overcome this limitation, we introduce a novel importance score extrapolation framework that requires training on only a small subset of data. We present two initial approaches in this framework¹—k-nearest neighbors and graph neural networks—to accurately predict sample importance for the entire dataset using patterns learned from this minimal subset. We demonstrate the effectiveness of our approach for 2 state-of-the-art pruning methods (Dynamic Uncertainty and TDDS), 4 different datasets (CIFAR-10, CIFAR-100, Places-365, and ImageNet), and 3 training paradigms (supervised, unsupervised, and adversarial). Our results indicate that score extrapolation is a promising direction to scale expensive score calculation methods, such as pruning, data attribution, or other tasks.

1 Introduction

In recent years, the demand for large and comprehensive datasets has grown rapidly. This is particularly evident in the development of advanced models, such as large language models (LLMs) [1], and other forms of foundation models [2, 3, 4], which require vast amounts of data to train.

In this context, dataset pruning has emerged as a valuable technique to optimize the training process and improve the efficiency of model development. By scoring individual data points by their importance and only selecting the most informative, dataset pruning aims to improve training efficiency while maintaining model performance. This approach is particularly beneficial in scenarios where the available dataset is vast, and the computational resources required for training the model on the entire dataset are significant, such as autonomous driving [5, 6].

However, existing pruning approaches generally require training a model on the full dataset to calculate data importance scores [7, 8]. As full, large-scale training runs are often conducted only once for a specific model, the effort required for this initial full-dataset training will often exceed the benefits gained from the pruning process, rendering the approach impractical.

To address this limitation, we propose a framework for score extrapolation. Our framework limits the expensive score computation to a small initial subset of the full training data. Subsequently, we

[†]These authors contributed equally to this work.

Corresponding authors sebastian95.schmidt@tum.de, prasanga.dhungel@tum.de

¹<https://github.com/prasangadhungel/Data-Pruning-with-Extrapolated-Scores>

extrapolate scores from the small subset to the entire dataset. By *avoiding the need for a full-dataset training*, score extrapolation substantially accelerates the dataset pruning and enables it for practical applications. Beyond immediate pruning applications, our findings suggest that importance score extrapolation offers a scalable approach that may be applied to other techniques involving expensive per-sample evaluations, including data attribution methods [9] or influence estimation [10].

Our contribution can be summarized as follows:

- We provide a novel framework for score extrapolation, which can be used to extrapolate expensive score extrapolation methods to unseen data samples, *significantly reducing computational effort*.
- In the scope of this framework, we introduce two extrapolation techniques based on k-nearest-neighbors (KNN) and graph neural networks (GNN).
- In an extensive empirical study, we showcase the effectiveness of our extrapolation-based approaches for **2** state-of-the-art pruning methods, i.e., Dynamic Uncertainty (DU) [7], Temporal Dual-Depth Scoring (TDDS) [8], **4** datasets (CIFAR-10 [11], CIFAR-100 [11], Places-365 [12], ImageNet [13]), and **3** different training paradigms (supervised, unsupervised, adversarial).

2 Related Work

Data pruning is usually costly to apply, as it requires either a full training or costly optimizations. We review the literature on data pruning in supervised and adversarial training.

Data Pruning. Data pruning, or coreset selection [7, 14, 15, 16, 17, 18], aims to keep a small, representative subset of training data that preserves model performance while reducing computational costs, which is specifically important when training is costly [19, 20, 21]. Several efficient strategies have emerged, which can be grouped into three categories [22] and either estimate importance or difficulty scores, use geometric calculation, or employ optimization. Importantly, approaches usually require full training on the dataset [7, 15, 23] to estimate importance scores or to create a latent space for pruning.

Pruning Based on Importance. Methods from this category assign scores to samples based on their utility for training, typically retaining the highest-ranked examples. Common techniques include GradNd [24] or TDDS [8] and rely on gradients, while others, like EL2N [24], use prediction errors of the model instead. Coleman et al. [25] use the entropy from proxy models for ranking, while forgetting scores track transitions between correct and incorrect classifications, suggesting that frequently forgotten samples are informative. AUM [26] identifies mislabeled measures by the average margin between the true class logit and the highest logit. DU [7] assesses uncertainty through the standard deviation of predictions during training.

An alternative approach measures importance by the impact of sample removal. The memorization score evaluates changes in confidence for the true label with and without the sample. The MoSo [22] score calculates the change in empirical risk, while [17, 27] use influence functions [10] to gauge the influence of a sample on generalization performance. While this category of pruning approaches is usually the most effective, it comes with a costly full dataset training to estimate the pruning scores.

Pruning Based on Geometry. Other approaches utilize geometric properties or the distribution of the data. Herding [28, 29] and Moderate [30] calculate distances in feature space. Some approaches [31, 32] combine gradients with distance calculations.

For instance, [33] constructs a coreset by approximating the maximum margin separating hyperplane. Self-Supervised Pruning [14] applies k -means clustering in the embedding space of a self-supervised model and ranks samples by their cosine similarity to cluster centroids, retaining samples with the lowest similarity. The k -center method [16] selects centers that minimize the maximum distance between any sample and its nearest center. Coverage-based approaches [34, 35] aim to maximize sample diversity while minimizing redundancy.

Pruning Based on Optimization. Some methods formulate pruning as an optimization problem. Borsos et al. [36] used greedy forward selection to solve a cardinality-constrained bilevel optimization problem for subset selection. GLISTER [37] performs coreset selection via a greedy-Taylor approx-

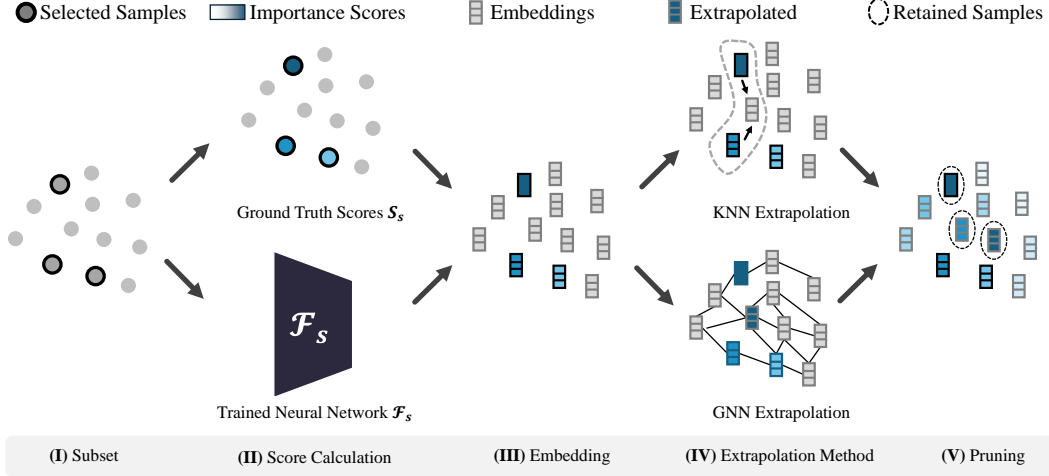


Figure 1: Extrapolation concept overview. (I) We start by randomly selecting a subset \mathbb{D}_s of m samples out of the full dataset \mathbb{D} comprising n samples (where $m < n$). (II) We train a neural network F_s on the selected subset and calculate ground truth importance scores S_s with the selected pruning method during the training run. (III) Using the trained model, we map the whole dataset \mathbb{D} to the embedding space of the network. (IV) Subsequently, we select an extrapolation method and train it to extrapolate scores on \mathbb{D}_s and the calculated ground truth scores S_s . (V) Finally, we use the original and extrapolated scores to perform the pruning task, selecting the top-k samples exhibiting the highest importance scores.

imation of a bilevel objective while simultaneously updating model parameters. GradMatch [38] defines a gradient error term and minimizes it using the Orthogonal Matching Pursuit algorithm.

Adversarial Robustness. Adversarial training [39, 40, 41, 42, 43] and other robustification methods [44, 45, 46, 47], generally involve expensive optimization [39, 48, 49, 50, 51], and thus entail large computational overhead. Yet, data pruning in adversarial training remains relatively under-explored. Existing approaches can be grouped into three broad categories. The first focuses on dynamically selecting which samples to apply adversarial perturbations to during training [52, 53]. The second incorporates coreset-based pruning methods to reduce training data while preserving robustness [54, 55]. The third relies on heuristic pruning strategies to discard samples deemed less useful for robust learning [56, 57].

Orthogonal Works. Beyond data pruning, identifying important subsets of data is a fundamental problem in various machine learning paradigms, including continual learning [58], data distillation [59, 60], and active learning [61, 62, 63, 64, 65]. While active learning focuses on selecting samples to label, data pruning addresses the challenge of selecting which samples to retain for training.

While data pruning methods lead to effective data reduction, approaches usually require training on the full dataset or complex optimization to estimate which samples to prune. Only a few works consider the time-of-accuracy problem to increase time efficiency, including RS2 [66], which proposes repeated random sampling, [67] selects data online during training by gradient evaluations or uses proxy models [25]. Here, we extend our previous short paper [21] and address the prohibitively expensive training on the full datasets is an unaddressed problem, which we address in this work.

3 Score Extrapolation

Existing methods [7, 15, 24] in the area of data pruning require complete training on the full dataset or rely on costly optimizations [37], which makes them prohibitively expensive.

To address the computational challenges of estimating data importance scores for large-scale data sets, we propose a score extrapolation framework. Within this framework, we compute the importance scores on *only* on a minor subset of the large-scale dataset and extrapolate scores for the remaining data points efficiently. The concept is shown in Figure 1 and comprises the following steps: At first, a subset of the large-scale dataset is selected (I). Based on this subset, a model is trained to calculate importance scores based on a chosen extrapolation method (II). To extrapolate the scores of the

remaining samples, we generate the embeddings of the dataset based on the trained model (III). With the calculated scores of the subset and the embeddings, we use one of the proposed extrapolation methods based on either KNN or a GNN (IV) to estimate scores for the remaining samples. In the last step (V), we perform the regular pruning task with our extrapolated scores.

Subset Definition. Rather than directly calculating the importance score for each sample in the dataset, we start by selecting a training subset $\mathbb{D}_s \subset \mathbb{D}$ of cardinality m from the full dataset \mathbb{D} , comprising n samples, where $m \ll n$. Our goal is to extrapolate data importance scores for the residual set $\mathbb{D}_r = \mathbb{D} \setminus \mathbb{D}_s$ containing the remaining $n - m$. We do not assume specific knowledge about our dataset \mathbb{D} and therefore use random sampling for generating \mathbb{D}_s .

Score Calculation and Model Training. Next, we select a suitable data pruning method from which to extrapolate scores. The choice of pruning method is critical, as the quality of extrapolated scores is inherently upper-bounded by the chosen method. We then train a model \mathcal{F}_s on the training subset \mathbb{D}_s , using the same setup as the pruning method would normally use for the full dataset. Through the training process, we obtain “ground truth” data importance scores $S_s \in \mathbb{R}^m$ for the subset \mathbb{D}_s .

Score Extrapolation. Based on the initial computed scores S_s , we apply an extrapolation schema to generate the scores $S_r \in \mathbb{R}^{n-m}$ for the residual set \mathbb{D}_r . In this work, we propose two extrapolation schemes: a basic KNN approach and a more advanced interpolation based on GNNs. Both concepts are illustrated in Figure 1. Finally, all samples in \mathbb{D} are assigned importance scores: samples in \mathbb{D}_s retain their directly computed values, while scores for \mathbb{D}_r are inferred. Once scores are computed for the full dataset, they can be used in the respective downstream tasks. In this work, we specifically focus on data pruning. However, the general framework could also be applied to other settings, such as data attribution [9], influence functions [10].

This strategy significantly reduces the computational cost of scoring large datasets. Instead of training on the full dataset, scores are computed only on a small subset, while the remaining samples are efficiently approximated through extrapolation.

3.1 Extrapolation with KNN

In the following, we propose two methods to extrapolate scores. First, as our baseline, we propose a simple KNN-based approach to estimate the importance scores. We start from the subset \mathbb{D}_s and its associated importance scores S_s . Next, we utilize the encoder of our trained model $\mathcal{F}_s : \mathbb{R}^d \rightarrow \mathbb{R}^{d'}$ to transform d dimensional input samples $x \in \mathbb{R}^d$ into the d' -dimensional embedding space of the encoder. Then, we compute the score for each data point $x \in \mathbb{D}_r$ as the average of the scores of its k nearest neighbors in the embedding space. Finally, the extrapolated importance score S_{knn} for a sample x can be expressed as

$$S_{knn}(x) = \frac{\sum_{i=1}^k \exp(-D(\mathcal{F}_s(x), \mathcal{F}_s(x_{\pi_i(x)}))) S_{\pi_i(x)}}{\sum_{i=1}^k \exp(-D(\mathcal{F}_s(x), \mathcal{F}_s(x_{\pi_i(x)})))}, \quad (1)$$

where $\pi_i(x)$ represents the index of the i -th nearest neighbor of x , and $D(\cdot, \cdot)$ denotes a chosen distance metric (i.e., Euclidean distance). This weighted average, based on the structure of the embedding space, ensures that the extrapolated scores maintain the local structure of the dataset.

3.2 Extrapolation with GNN

While KNN-based extrapolation serves as a simple approach to extrapolate information from the sampled subset \mathbb{D}_s to the residual data \mathbb{D}_r , it lacks the ability to model complex interactions among data points. To address this limitation, we additionally propose a more powerful extrapolation method based on GNNs that can capture higher-order relationships in the dataset through message passing. We construct an undirected graph $\mathcal{G} = (\mathcal{V}, \mathcal{E})$, where each sample in \mathbb{D} represents a vertex in \mathcal{V} , and edges \mathcal{E} are formed between each sample and its k nearest neighbors in the embedding space. The node embeddings are defined based on the sample embeddings of the model \mathcal{F}_s and are combined with the one-hot encoded class labels for supervised tasks.

In addition, we define edge weights based on the latent space distance to its neighbors encoded as $\exp(-d(\mathcal{F}_s(x), \mathcal{F}_s(x_{\pi_i(x)})))$. The adjacency matrix \mathcal{A} is constructed based on these edges.

To learn the interactions between the data samples, we employ a simple GNN $\mathcal{F}_{\mathcal{G}}(\mathcal{A}, \mathcal{V}; \theta)$ with weights θ that consists of three layers of Graph Convolutional Networks (GCNs) as described by [68]

and directly predicts the importance score of the sample nodes given our defined node embeddings \mathcal{V} and adjacency matrix \mathcal{A} .

To scale training in large graphs, we employ neighbor sampling [69] to generate mini-batches of nodes and their local neighborhoods during training.

Importantly, GNNs are significantly less computationally expensive than the task model, which we analyze in our experiments. The GNN outputs a vector of predicted scores \mathbb{R}^n , i.e., a scalar score for each node. Since we only have the reference score $S_s(x)$ for samples in the training dataset \mathbb{D}_s , we compute the mean square loss only over these nodes as

$$\mathcal{L} = \frac{1}{|\mathbb{D}_s|} \sum_{x_i \in \mathbb{D}_s} (\mathcal{F}_G(\mathcal{A}, \mathcal{V}; \theta)_i - S(x_i))^2, \quad (2)$$

where $\mathcal{F}_G(\mathcal{A}, \mathcal{V}; \theta)_i$ is the prediction for index i . After training, we use the GNN to infer scores for all samples in $\mathbb{D} \setminus \mathbb{D}_s$. The message passing in the GNN allows the model to leverage the structural information of the entire dataset, potentially leading to more accurate extrapolation of the scores.

4 Evaluation

In the following section, we aim to evaluate our importance score extrapolation for different scores, tasks, and datasets. The primary objective of this paper is to evaluate the practical feasibility of score extrapolation. We present this as foundational research that characterizes the approach’s strengths and limitations, upon which future optimization efforts can build. Our experiments are designed to analyze the core properties of the method rather than to maximize performance metrics. We have three main goals for score extrapolation: 1) *reduce* the computation time compared to standard pruning, 2) *maintain* downstream task performance, and 3) show high *correlation* to the original scores which are generated by training a model and estimating the scores on the full set \mathbb{D} . To examine these properties, we evaluate the tasks of classic data pruning for labeled data, unsupervised data pruning, and adversarial training.

Scores. In our experiments, we extrapolate two state-of-the-art pruning methods, DU [7] and TDDS [8]. Both methods require training on the full dataset for several epochs to obtain reliable scores. They also store logits per sample at each epoch; DU retains only the softmax logits for the correct class, whereas TDDS approximates gradients from full logit outputs, making it more memory-intensive. Details on these scores are provided in Appendix B.

Supervised Data Pruning. We first evaluate score extrapolation on supervised data pruning. The objective of this task is to minimize the amount of training data while maintaining model performance as much as possible. Since we focus on large datasets, we use synthetic CIFAR-100 1M [11, 41], Places 365 [12], and ImageNet 1k [13]. We compare our extrapolated scores with the original pruning approaches and random pruning and examine the different initial subset sizes \mathbb{D}_s ranging from 10%, to 25%. If not stated otherwise, we use 20% of the full dataset for \mathbb{D}_s in all experiments. More details are given in Appendix A. All experiments were conducted with 3 different random initializations.

Table 1 illustrates the effect of our extrapolation schemes across the different datasets and pruning approaches. As expected, the results indicate that the extrapolated scores perform slightly worse than the original scores. However, score extrapolation is considerably faster in our experiments, while requiring less data for initial model training. The time measurement contains *all* steps, including the training of the model for initial scores S_s , possible extrapolation approaches, and the training of the final model on the pruned subset.

Notably, the medium-sized training subsets \mathbb{D}_s demonstrate strong performance, while the small subset already shows decent results and generally outperforms random pruning. GNN-based extrapolation generally performs better than using KNN. Still, KNN extrapolation is *pareto optimal* w.r.t. time-accuracy trade-offs (see Time Optimality).

Pruning Performance. In Figure 2 we compare pruning strategies at different pruning rates. The difference in final accuracy between ground truth scores to extrapolation methods is low for Places365 (Figure 2a) and ImageNet (Figure 2b). While TDDS maintains a higher accuracy for moderate pruning

rates, the difference to our extrapolation decreases for higher pruning rates. DU performs worse than random pruning for pruning rates over 50%, making comparisons in this regime irrelevant.

For synthetic CIFAR-100 1M, the original DU and TDDS actually improve model accuracy compared to standard training. We attribute this to the ability of the pruning methods to filter out noisy data. Similarly, score extrapolation techniques demonstrate performance gains over standard training, though the effect is less substantial than with direct pruning methods.

For the smaller CIFAR-10 (Figure 2d), the performance between ground truth scores and extrapolated ones is identical for TDDS up to 20% pruning. Importantly, across all datasets, extrapolated scores consistently outperform random pruning whenever the ground truth score does, demonstrating the practical value of score extrapolation.

Time Optimality. We examine the computational behavior of the extrapolation approaches in more detail. While the original scores demonstrate higher accuracy, indicating an upper bound for the extrapolation methods, their calculation is costly. Figure 3 compares the model performance with the pruning and training time. We see that our extrapolated scores, especially the KNN extrapolation, are always Pareto optimal for Places365 and ImageNet. In contrast, the standard pruning approaches require more time for the standard pruning than even a regular full training. They would only obtain any real-time advantage if multiple unpruned training runs were to be performed, while our extrapolated scores provide a time advantage already at the first run.

Relationship between Score Correlation and Downstream Task Performance. To verify the results presented in the Table 1, we examine the correlation between the extrapolation and the original scores. Table 2 reports Pearson [70] and Spearman [71] correlation. As expected, the correlation increases with the subset size. We already saw that a 10% subset size is sufficient for high performance in the pruning task in previously presented results. In addition, the GNN’s correlation is always higher than the KNN’s, underlining the GNN’s greater ability to capture dataset properties.

As the next step, we investigated the actual relationship of these correlation scores to the downstream task performance. In Figure 4, we show the Pearson and Spearman correlation over the accuracy. The correlation of the original and extrapolated scores perfectly aligned with achieved accuracy, confirming the obtained pruning results of our extrapolated scores.

Table 3: Pearson and Spearman correlations for unsupervised extrapolation for CIFAR10 with DU based on the Turtle [72].

Subset size	Pearson ρ		Spearman r_s	
	GNN	KNN	GNN	KNN
20%	0.4201	0.5481	0.5312	0.6630
10%	0.3692	0.5078	0.4519	0.6211

Unsupervised Data Pruning. Since our extrapolation paradigm works effectively for classic data pruning, we modify the labeled data constraints of data pruning to investigate the flexibility and scalability of our approach. When dealing with large datasets, the assumption that all data is labeled might not be realistic. Thus, we modify the

Table 1: Accuracy (\pm std. error) and inference time (\pm std. error, in minutes) for various datasets, at the highest pruning percentages, where the pruning algorithms still outperform random pruning. Small subset corresponds to 10% of the initial dataset, while medium corresponds to 20% for Synthetic CIFAR and ImageNet and 25 % for Places365.

Dataset	Prune %	Method	Original	GNN Medium Set	KNN Medium Set	GNN Small Set	KNN Small Set	Random
Imagenet	50	DU	59.08 \pm 0.07	58.89 \pm 0.16	58.74 \pm 0.14	58.30 \pm 0.17	58.51 \pm 0.14	58.56 \pm 0.06
			1367 \pm 19	829 \pm 15	687 \pm 16	701 \pm 12	581 \pm 10	
Places365	50	DU	42.85 \pm 0.09	42.51 \pm 0.14	42.30 \pm 0.12	42.32 \pm 0.13	42.36 \pm 0.11	42.14 \pm 0.09
			2416 \pm 26	1631 \pm 18	1330 \pm 14	1394 \pm 15	1075 \pm 13	
Places365	95	TDDS	34.61 \pm 0.17	33.96 \pm 0.26	33.56 \pm 0.19	33.58 \pm 0.21	33.29 \pm 0.18	32.89 \pm 0.13
			1741 \pm 22	917 \pm 17	621 \pm 13	668 \pm 11	353 \pm 8	
Synthetic CIFAR-100	95	DU	71.42 \pm 0.21	69.62 \pm 0.26	69.13 \pm 0.22	68.60 \pm 0.24	68.81 \pm 0.23	67.38 \pm 0.19
			412 \pm 9	374 \pm 6	158 \pm 5	333 \pm 6	114 \pm 5	
Synthetic CIFAR-100	95	TDDS	72.51 \pm 0.18	71.16 \pm 0.28	70.80 \pm 0.24	69.24 \pm 0.22	69.10 \pm 0.21	67.38 \pm 0.20
			441 \pm 10	387 \pm 6	168 \pm 6	343 \pm 7	122 \pm 5	

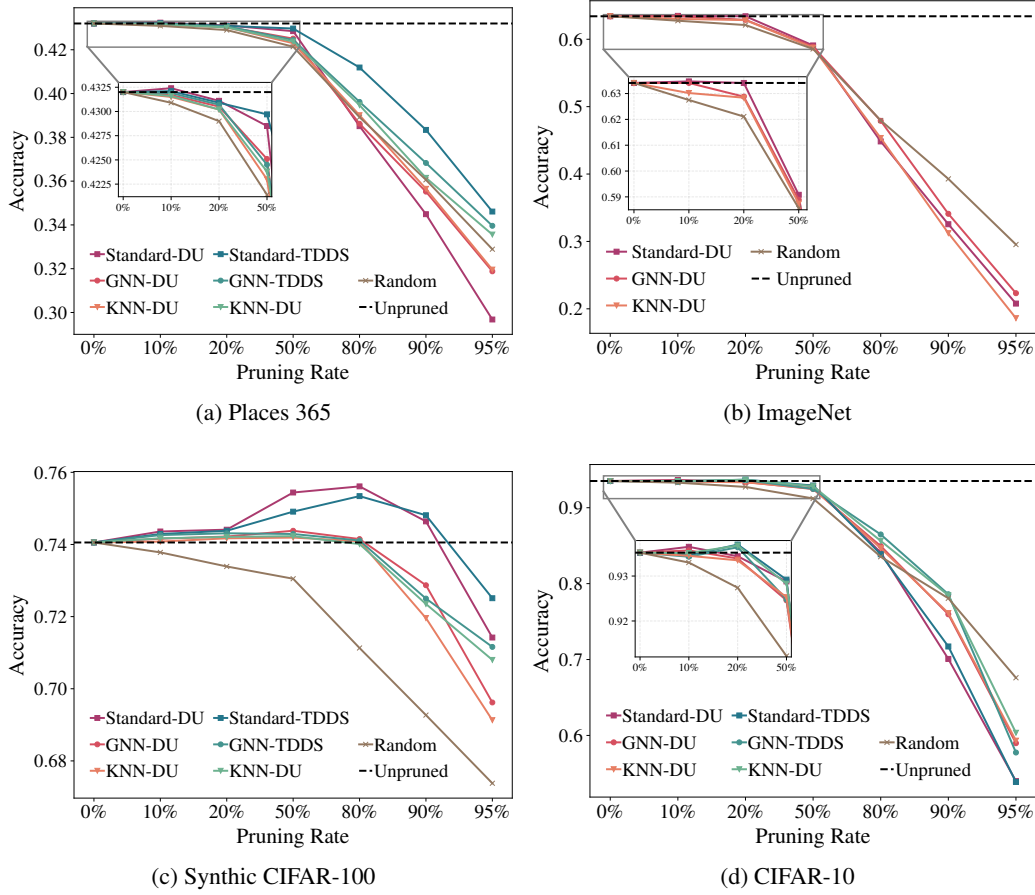


Figure 2: Evaluation of accuracy for different pruning rates and different datasets. Experiments are averaged over three seeds. In most setups, the GNN extrapolation scores outperform the KNN extrapolation. Especially for low pruning rates, the difference to the original pruning approach is quite low.

original data pruning task to work with unlabeled datasets. We use Turtle [72] for the unsupervised image classification on CIFAR-10, and applied the score calculation with DU and our extrapolations. Further experiment details can be found in Appendix A.

For our newly created unsupervised data pruning setup, we focus on analyzing the correlation of our extrapolation approaches to the original DU score. In Table 3 we can see that the correlations of the extrapolated scores are as high as for the standard pruning approach, indicating the flexibility of the extrapolation paradigm. Interestingly, KNN has a higher correlation than GNN. Which might be caused by the foundation model defined latent space that Turtle uses. In addition, the correlation increases with the size of the subset.

Adversarial training. In addition to the supervised and unsupervised, we investigate the adversarial training scenario, where our extrapolation can confirm its high effectiveness in selecting a subset for adversarial training. We perform adversarial training in the ℓ_∞ -norm with a perturbation budget of $\epsilon = 8/255$ on the CIFAR-10 [11] dataset. We use the same training hyperparameters as in [41]. In each case, we prune 25% of the data. Table 4 summarizes the robustness for the different methods. Score extrapolation considerably improves upon random pruning in terms of robustness and model accuracy on clean data. As expected, it performs only slightly worse than using ground truth scores directly. The KNN extrapolation approach achieves 0.54 linear correlation with the ground truth scores, which could be improved by more sophisticated extrapolation approaches.

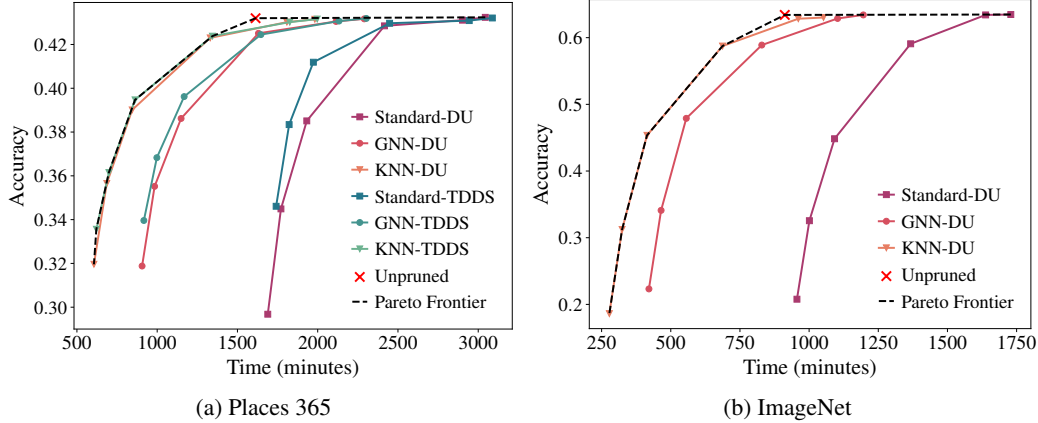


Figure 3: Pareto plots of time to accuracy behavior for different pruning methods and the full dataset training. It can be seen that the pruning approaches are always slower than our extrapolation approach, while high pruning rates show faster than full training behavior.

Table 2: Pearson and Spearman correlations for different pruning methods across datasets. GNN always achieves a higher correlation than KNN, and both approaches increase correlation with a higher training subset.

Dataset	Method	Subset size (%)	Pearson ρ		Spearman r_s	
			GNN	KNN	GNN	KNN
Imagenet	DU	20	0.4193	0.3779	0.3503	0.3068
		10	0.2850	0.2575	0.2178	0.1980
Places365	DU	25	0.4004	0.3081	0.3611	0.2524
		10	0.2612	0.2215	0.2158	0.1791
	TDDS	25	0.2632	0.2251	0.2646	0.2214
		10	0.2372	0.1620	0.2297	0.1594
Synthetic CIFAR	DU	20	0.4910	0.4538	0.7009	0.6562
		10	0.3396	0.3243	0.5593	0.5471
	TDDS	20	0.4236	0.3955	0.6713	0.6244
		10	0.3849	0.3273	0.5722	0.5324

In Table 5, we additionally provide results for KNN-based extrapolation for a larger dataset. Here, we also evaluate our approach for ℓ_2 -based adversarial training ($\epsilon = 128/255$). We extrapolate scores from the DU scores from a standard CIFAR-10 training run to 2 million synthetic CIFAR-10 images from [41] and prune 50% of the data. We do not compare to pruning with ground truth scores, as performing a full adversarial training run with 2 million data samples was too expensive. Score extrapolation outperforms random pruning in both settings, while introducing only negligible computational overhead ($< 6\%$). This result demonstrates the effectiveness of score extrapolation in

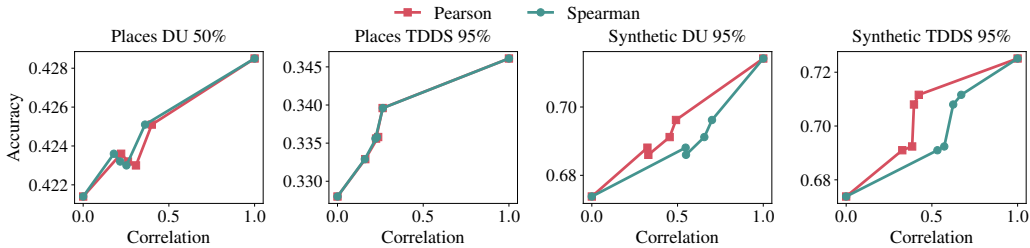
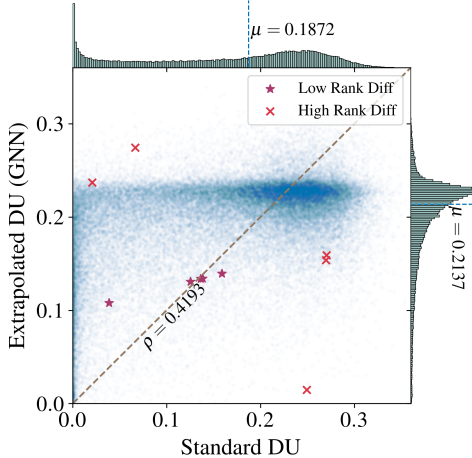


Figure 4: Analysis of the dependency of correlation and accuracy of the extrapolation methods for Places365 and synthetic CIFAR-100. The accuracy increases with the correlation of the specific task.



(a) Correlation of Scores



(b) High rank difference examples



(c) Low rank difference examples

Figure 5: Score distribution (a) and qualitative analysis (b-c) of extrapolation errors for ImageNet and DU. a) Extrapolated scores show a moderate correlation with ground truth but miss the bimodal structure, resulting in a narrower, oversmoothed distribution. (b) and (c) show examples with high and low rank discrepancies. High discrepancies often correspond to outliers with atypical backgrounds or multiple objects, while low discrepancies align with prototypical class examples.

adversarial training, when the initial seed dataset is considerably smaller than the full dataset (i.e., $m \ll n$).

Table 4: Comparison of the utility of original and extrapolated DU scores on the CIFAR-10 dataset for ℓ_∞ -norm adversarial training ($\epsilon = 8/255$). 25% of the samples are pruned for each method. Random pruning is provided as a baseline.

Experiment	Robust	Clean
Random	47.95%	80.43%
Extrapolated-KNN	50.39%	80.86%
Ground Truth Scores	52.26%	81.95%

Table 5: Evaluation of extrapolated DU scores on a 2 million sample synthetic CIFAR-10 dataset. 50% of the 2 million synthetic samples are pruned for each method. We provide random pruning as a baseline.

NORM	EXPERIMENT	ROBUST	CLEAN
ℓ_2	RANDOM	80.79%	94.20%
	EXTRAPOLATED KNN	81.28%	94.22%
ℓ_∞	RANDOM	63.13%	90.86%
	EXTRAPOLATED	63.56%	90.50%

Limitations and Visual Analysis. In Figure 5 (a), we perform a deeper investigation regarding limitations of our extrapolation approach, superficially focusing on extrapolated DU scores on the ImageNet dataset. While the extrapolation method achieves a moderate correlation between ground truth and estimated scores, the extrapolated scores fail to capture the bimodal structure present in the original distribution, instead forming a narrower, unimodal distribution with a higher mean and lower variance. This oversmoothing likely contributes to the observed extrapolation errors.

To further investigate these errors, we highlight samples with high and low rank differences (specifically using one "dog" class, but other classes showed similar patterns). Qualitative examples in subfigures (b) and (c) suggest that high rank differences often correspond to atypical or out-of-distribution samples—such as those with unusual backgrounds, multiple subjects, or low visual quality—whereas low rank difference samples tend to be prototypical, centered, and consistent in appearance. This indicates that the extrapolation method struggles most with outliers and visually ambiguous inputs. We hypothesize that more powerful extrapolation methods or using more seed data to train the score extrapolation would improve score extrapolation in these cases.

5 Conclusion

Since data pruning usually requires a full training on the dataset to estimate the scores for a subset selection, its applicability to large-scale datasets and real-world applications is limited. To mitigate this problem, we propose a novel score extrapolation paradigm. Instead of training on the full set, we select a small subset to estimate the initial scores for the chosen data pruning method and extrapolate these scores to the remaining samples in the dataset using a computationally efficient extrapolation method. In this work, we propose a KNN- and a GNN-based extrapolation scheme, which are easily applicable to different learning tasks. Our experiments show that the extrapolated scores show high correlation with the original scores and achieve a high downstream task performance for two different pruning scores, three different tasks, and four different datasets. A closer look at the extrapolation errors shows that our initial methods fail to capture the full complexity of the ground truth score distributions. A visual investigation reveals that extrapolation is particularly challenging for outlier samples that deviate from prototypical class examples.

Outlook. In future work, we aim to improve downstream task performance, which could include increasing extrapolation accuracy, for example, by refining the GNN-based score estimator, exploring new extrapolation methods, and investigating alternative subset selection strategies. Moreover, we aim to extend our extrapolation approach to other data selection tasks involving costly score computations, such as influence functions [10] and data attribution [9]. Finally, we believe score extrapolation could also benefit tasks beyond data selection, such as out-of-distribution detection.

Acknowledgments and Disclosure of Funding

This research was supported and partially funded by Pontificia Universidad Católica de Valparaíso, Vice Rector’s Office for Research, Creation and Innovation within the programs "DI Iniciación" (039.485/2024) and "Semilla 2023" (039.247)

A Experiment Setup

A.1 Dataset

To evaluate the efficacy of our proposed score extrapolation framework, we conduct experiments on four image classification datasets differing in scale, number of classes, and image resolutions: CIFAR-10 [11] (50K samples, 10 classes, 32×32), synthetic CIFAR-100 [41] (1M samples, 100 classes, 32×32 , generated with denoising diffusion models [73]), Places-365 [12] (1.80M samples, 365 classes, resized to 64×64 to expedite experiments), and Imagenet-1k [13] (1.28M samples, 1000 classes, downsampled version of 64×64). To evaluate model accuracy after pruning, we use the original test sets of each dataset, with the exception of synthetic CIFAR-100, for which we employ the standard CIFAR-100 [11] test set. Additionally, we explore the unsupervised dataset pruning with standard CIFAR-10, and adversarial training with synthetic CIFAR-10 [41] (2M samples).

Dataset License: All datasets used in our experiments are publicly available, and most of them are widely used in the ML community. The standard CIFAR-10 and CIFAR-100 [11] datasets are freely available for research and educational purposes without any licensing requirements. ImageNet [13] is available for free to researchers for non-commercial use but does not outline a specific license. Both synthetic CIFAR-10 and synthetic CIFAR-100 [41]² are publicly available under the MIT license. Similarly, Places365 [12] is released under the MIT license. We performed experiments adhering to the licensing terms of the respective datasets.

A.2 Statistical Significance

Since the computed scores depend on the training, which is stochastic by nature, the scores obtained at the end are also stochastic. To ensure statistical robustness, for any dataset, we compute three different sets of ground truth scores $S \in \mathbb{R}^n$ with three different random initializations. For each set of scores, we compute the model accuracy at various pruning rates: 10, 20, 50, 80, 90 and 95 percentages. To compute subset scores S_s , we follow the same procedure. We randomly select $\mathbb{D}_s \subset \mathbb{D}$ of cardinality m , and compute the scores S_s with standard pruning algorithms. We do this three times with three different seeds. For each set of S_s , we extrapolate using the KNN and GNN approaches. In this way, we obtain six sets of extrapolated scores S_r , (three from KNN, and three from GNN). Note that extrapolation with GNN itself is stochastic in nature. For each set of scores, we prune the data at various rates and train the model on the pruned dataset once. Thus, for each pruning rate, we get three test accuracy values for both extrapolation methods. Figure 2, Figure 6 and Figure 3 report this mean accuracy.

A.3 Computational Resources

All experiments are conducted using NVIDIA A100-PCIE GPUs, with 42.4 GB of VRAM. Computational time reported in Table 1, and Figure 3 are the total mean runtime (in minutes) required to compute S_s , extrapolate, and subsequent model training on the pruned dataset. Time for ground truth scores reflects the mean time required for full dataset scoring plus training on the pruned subset.

A.4 Models

Both DU, and TDDS require model training for numerous epochs to compute the scores. To validate that score extrapolation works with different models \mathcal{F}_s , we used ResNet-18 [74] for Cifar-10, and Imagenet, and ResNet-50 for Synthetic CIFAR-100, and Places-365. For the adversarial setting, we used Wide-ResNet-28-10 [75]. During extrapolation, samples are represented in the embedding space induced by these models.

For the unsupervised setting, we employ DINOv2 [76] as a foundation model to obtain fixed embeddings for all samples. Both extrapolation procedures (KNN-based and GNN-based) are subsequently performed in the embedding space of this foundation model. This diversity of architectures and training paradigms demonstrates that our extrapolation approach is not restricted to a specific model but can be applied broadly across a range of backbone networks and training schemes.

²<https://github.com/wzekai99/DM-Improves-AT/>

A.5 Experiment Hyperparameters

We collected all hyperparameter setting in Tables 6 to 9. They are properly introduced with the scored description in the following section.

B Scores

We assess our extrapolation framework with two state-of-the-art dataset pruning methods: Dynamic Uncertainty (DU) [7], and Temporal Dual-Depth Scoring (TDDS) [8].

B.1 DU Scores

Given a model θ_k trained over K epochs, $U_k(x)$ for a sample x at epoch k is computed as the standard deviation of the predicted probabilities $\mathbb{P}(y|x, \theta_k)$ over a sliding window of J epochs [7]:

$$S_k(x) = \sqrt{\frac{1}{J-1} \sum_{j=0}^{J-1} [\mathbb{P}(y|x, \theta_{k+j}) - \bar{\mathbb{P}}]^2},$$

where $\bar{\mathbb{P}} = \frac{1}{J} \sum_{j=0}^{J-1} \mathbb{P}(y|x, \theta_{k+j})$. The final dynamic uncertainty score $S(x)$ for each sample is computed by averaging over all sliding windows:

$$S(x) = \frac{1}{K-J} \sum_{k=0}^{K-J-1} S_k(x),$$

For experiments, we set $J = 10$, and $K = 50$ for CIFAR-10, synthetic CIFAR-100 and PLACES-365, while $K = 90$ is used for Imagenet. More details on the hyperparameters are provided in Table 6.

B.2 TDDS Scores

TDDS [8] computes the importance score for a sample x by quantifying its contribution to optimization dynamics. Specifically, TDDS calculates the epoch-wise change in loss, $\Delta\ell_k(x)$, projected onto the model’s optimization trajectory. Formally, for a sliding window of size K , the score is computed as:

$$S(x) = \sum_{k=J}^K \beta(1-\beta)^{K-k} \sum_{j=k-J+1}^k \left(|\Delta\ell_j(x)| - \frac{1}{J} \sum_{i=k-J+1}^k |\Delta\ell_i(x)| \right)^2,$$

where $\Delta\ell_k(x)$ measures the KL-divergence of predictions between consecutive epochs:

$$\Delta\ell_k(x) = f_{\theta_{k+1}}(x)^\top \log \frac{f_{\theta_{k+1}}(x)}{f_{\theta_k}(x)},$$

and β is an exponential decay factor. In experiments, we set $J = 10$, and $\beta = 0.9$ for all datasets, and $K = 50$ for CIFAR-10, synthetic CIFAR-100, and Places-365, whereas $K = 90$ for ImageNet. Further details are provided in Table 7.

B.3 Unsupervised DU Scores

To assess whether our score-extrapolation framework remains effective in the absence of ground-truth labels, we employ TURTLE [72]. TURTLE assigns a pseudo-label to each sample $x \in \mathcal{D}$ by optimizing a bilevel objective within the representation space induced by a foundation model ϕ .

During TURTLE optimization, at each outer iteration $k \in \{1, \dots, K\}$, we record the softmax probability vector:

$$\mathbf{p}^{(k)}(x) = \text{softmax} \left(\boldsymbol{\theta}^{(k)} \phi(x) \right) \in \Delta^{C-1},$$

where $\theta^{(k)}$ denotes the learnable linear transformation at iteration k , and C is the number of classes specified a priori. After K outer iterations, we define the final pseudo-label for x as

$$\hat{y}(x) = \arg \max_{c \in \{1, \dots, C\}} \mathbf{p}_c^{(K)}(x).$$

Analogous to the supervised setting, we perform post-hoc computation to obtain the uncertainty at the pseudo-label $\hat{y}(x)$ across a sliding window of length J over epochs and subsequently average these values to compute the *unsupervised-DU* score for each sample.

Similar to the supervised setting, we use $J = 10$ for the experiments. Further hyperparameter details are provided in Table 9, which follows settings in [8].

Table 6: Hyperparameters and experimental settings for all datasets to compute standard DU scores \mathbb{S} , as well as subset DU scores \mathbb{S}_s . Subset sizes are reported as a percentage of the total dataset size. To compute standard scores, training is done on the complete dataset

Hyperparameters	CIFAR-10	Synthetic CIFAR-100	Places-365	ImageNet
Num epochs (K)	50	50	50	90
Batch size (B)	256	256	128	256
Model (\mathcal{F})	ResNet-18 [74]	ResNet-50	ResNet-50	ResNet-18
Optimizer	Adam [77]	Adam	Adam	Adam
Learning rate (η)	10^{-3}	10^{-3}	10^{-3}	10^{-3}
Weight decay (λ)	10^{-4}	10^{-4}	10^{-4}	10^{-4}
Scheduler	None	None	None	None
Window (J)	10	10	10	10
Subset size (m)	40%, 20%	30%, 20%, 10%	25%, 10%	20%, 10%

Table 7: Hyperparameters to compute standard and subset TDDS scores.

Hyperparameters	CIFAR-10	Synthetic CIFAR-100	Places-365
Num epochs (K)	50	50	50
Batch size (B)	256	256	128
Model (\mathcal{F})	ResNet-18	ResNet-50	ResNet-50
Optimizer	SGD	SGD	SGD
Learning rate (η)	10^{-3}	10^{-3}	10^{-3}
Weight decay (λ)	5×10^{-4}	5×10^{-4}	5×10^{-4}
Momentum	0.9	0.9	0.9
Nesterov [78]	True	True	True
Scheduler	CosineAnnealing [79]	CosineAnnealing	CosineAnnealing
Window (J)	10	10	10
Trajectory	10	10	10
Exponential decay (β)	0.9	0.9	0.9
Subset size (m)	40%, 20%	20%, 10%	25%, 10%

B.4 Scores Extrapolation

For KNN-based extrapolation, we computed the k nearest neighbors using the Euclidean distance. To assess how the choice of k affects extrapolation, we varied k across 10, 20, 50, 100 and evaluated the correlation between the extrapolated and ground-truth scores (based on S) for samples in \mathbb{D}_r . The value of k , yielding the highest Pearson correlation, is reported in our main results (Table 2), while the full ablation is presented in Table 10.

For GNN-based extrapolation, we similarly examined the effect of the neighborhood size k while constructing the graph. We used different values of k (10, 20, and 50). The GNN comprises three GCN [68] layers (hidden dimensions 512 and 256) and an output layer producing scalar importance scores. We use dropout regularization of 0.5 to avoid overfitting. To ensure scalability on large dataset, we use neighbor sampling [69], with mini-batches of nodes size 128.

Table 8: Hyperparameters used for training models on pruned datasets. Both random pruning, and score based pruning (standard as well as extrapolated scores) use the same configurations

Hyperparameters	CIFAR-10	Synthetic CIFAR-100	Places-365	ImageNet
Num epochs (K)	50	50	50	90
Batch size (B)	256	256	128	256
Model (\mathcal{F})	ResNet-18	ResNet-50	ResNet-50	ResNet-18
Optimizer	Adam	Adam	Adam	Adam
Learning rate (η)	10^{-3}	10^{-3}	10^{-3}	10^{-3}
Weight decay (λ)	10^{-4}	10^{-4}	10^{-4}	10^{-4}
Scheduler	OneCycle [80]	OneCycle	OneCycle	OneCycle
Window (J)	10	10	10	10

Table 9: Hyperparameters to compute unsupervised DU scores (for full dataset, as well as subset)

Hyperparameters	CIFAR-10
Num epochs (K)	400
Batch size (B)	10,000
Inner steps (M)	10
Representation (ϕ)	DINOv2 [76]
Optimizer	Adam
Regularization coeff. (γ)	10
Inner Learning rate (η_{in})	10^{-3}
Outer Learning rate (η_{out})	10^{-3}
Weight decay (λ)	10^{-3}
Scheduler	None
Window (J)	10
Subset size (m)	40%

We randomly split m samples in \mathbb{D}_s into 90% training and 10% validation set. These nodes already have the computed scores S_s . We train GNN for 25 epochs, and the checkpoint achieving the highest Pearson correlation between predicted and reference scores (based on S_s) on the validation set is selected for inference. Scores for all samples in $\mathbb{D}_r = \mathbb{D} \setminus \mathbb{D}_s$ are inferred using this model checkpoint. We report the correlation between the inferred scores and scores with the standard approach (S) for the samples in \mathbb{D}_r .

Interestingly, we observe that GNNs usually achieved the best performance with smaller neighborhood sizes ($k = 10$), suggesting that message passing enables effective propagation of information even with sparse local connectivity. Detailed results are provided in Table 11, with the best-performing configuration reported in Table 2.

C Additional Experiments

C.1 Relationship between Correlation and Downstream Task Accuracy

We investigate whether higher Pearson (ρ) or Spearman rank (r_s) correlations between extrapolated and ground truth scores are indicative of improved pruning performance, particularly in regimes where ground truth pruning outperforms random pruning. For the highest pruning rate at which ground truth pruning yields superior accuracy to random pruning, we compare the downstream accuracies obtained by retaining top-scoring samples according to various scoring methods (extrapolated, standard, and random). Note that random pruning corresponds to 0 correlation, while ground truth scores correspond to perfect correlation ($\rho = 1$, $r_s = 1$). Our findings indicate that increased correlation between extrapolated and ground truth scores leads to downstream accuracies that closely match those of ground truth-based pruning (see Figure 4). We further quantify the relationship between correlation metrics and downstream accuracy (A) after pruning by computing the Pearson and Spearman correlations between these variables. Results are summarized in Table 12.

Table 10: Pearson and Spearman correlations for different k in KNN pruning methods across datasets.

Dataset	Method	Sample size (%)	Pearson ρ				Spearman r_s			
			$k=10$	$k=20$	$k=50$	$k=100$	$k=10$	$k=20$	$k=50$	$k=100$
Imagenet	DU	20	0.3764	0.3779	0.3698	0.3607	0.2911	0.3068	0.3057	0.2982
		10	0.2507	0.2572	0.2575	0.2513	0.1773	0.1888	0.1980	0.1894
Places365	DU	25	0.2904	0.3054	0.3081	0.3004	0.2283	0.2446	0.2524	0.2487
		10	0.2139	0.2196	0.2215	0.2184	0.1687	0.1722	0.1791	0.1715
	TDDS	25	0.2169	0.2208	0.2251	0.2213	0.2128	0.2180	0.2214	0.2159
		10	0.1497	0.1561	0.1620	0.1583	0.1438	0.1526	0.1594	0.1513
Synthetic	DU	30	0.4964	0.5092	0.5118	0.5106	0.6675	0.6864	0.6962	0.6955
		20	0.4447	0.4530	0.4538	0.4499	0.6355	0.6493	0.6562	0.6562
		10	0.3123	0.3197	0.3243	0.3202	0.5286	0.5374	0.5471	0.5438
	TDDS	20	0.3821	0.3886	0.3955	0.3910	0.6067	0.6122	0.6208	0.6197
		10	0.3096	0.3178	0.3273	0.3147	0.5137	0.5261	0.5324	0.5311
		10	0.3096	0.3178	0.3273	0.3147	0.5137	0.5261	0.5324	0.5311
CIFAR-10	DU	40	0.6149	0.6328	0.6371	0.6313	0.6225	0.6411	0.6477	0.6447
		20	0.2721	0.2759	0.2765	0.2762	0.2603	0.2597	0.2558	0.2507
	TDDS	40	0.3841	0.4126	0.4181	0.4158	0.5593	0.5898	0.6029	0.6040
		20	0.2014	0.2128	0.2134	0.2038	0.2738	0.2806	0.2764	0.2611

Table 11: Pearson and Spearman correlations for different k in GNN based extrapolation

Dataset	Method	Sample size (%)	Pearson ρ			Spearman r_s		
			$k=10$	$k=20$	$k=50$	$k=10$	$k=20$	$k=50$
Imagenet	DU	20	0.4193	0.4139	0.4045	0.3503	0.3442	0.3388
		10	0.2850	0.2734	0.2784	0.2178	0.2189	0.2159
Places365	DU	25	0.4004	0.3869	0.3798	0.3608	0.3443	0.3373
		10	0.2612	0.2604	0.2577	0.2158	0.2140	0.2095
	TDDS	25	0.2632	0.2615	0.2557	0.2646	0.2611	0.2559
		10	0.2372	0.2275	0.2219	0.2297	0.2238	0.2184
Synthetic	DU	30	0.5593	0.5606	0.5634	0.7300	0.7344	0.7281
		20	0.4910	0.4886	0.4829	0.7009	0.6983	0.6942
		10	0.3396	0.3320	0.3282	0.5593	0.5513	0.5472
	TDDS	20	0.4236	0.4193	0.4155	0.6713	0.6711	0.6673
		10	0.3849	0.3801	0.3763	0.5722	0.5715	0.5639
		10	0.3849	0.3801	0.3763	0.5722	0.5715	0.5639
CIFAR-10	DU	40	0.6163	0.6318	0.6197	0.6533	0.6608	0.6582
		20	0.4080	0.2853	0.2574	0.3915	0.3009	0.2619
	TDDS	40	0.3891	0.3217	0.3007	0.5656	0.4213	0.4076
		20	0.1763	0.1630	0.1571	0.2008	0.1120	0.1095

C.2 Pruning Performance with Smaller Subset Sizes

In Figure 2 we evaluated the pruning performance of Random Pruning, Standard pruning (DU, and TDDS), and extrapolation-based pruning with initial score computation on a subset of size $m = 20\%$ (25% for Places-365, 40% for CIFAR-10). Here we provide additional results examining the impact of reducing the initial subset size, specifically considering $m = 10\%$ (20% for CIFAR-10). The results are presented in Figure 6.

We observe that, consistent with the initial larger subset size (Figure 2), pruning with extrapolated scores, even with a smaller initial subset size, outperforms the random baseline whenever the respective standard scores do. However, as the initial subset size m decreases, the effectiveness of extrapolated scores diminishes. They also have smaller Pearsons correlation and Spearman rank with the standard score, as demonstrated in Tables 2, 10 and 11.

Table 12: Pearson (ρ) and Spearman (r_s) correlations of scores correlation between extrapolated and original scores, and post-pruning accuracy (A)

Dataset	Prune %	Method	$\rho(\rho, A)$	$\rho(r_s, A)$	$r_s(\rho, A)$	$r_s(r_s, A)$
Places365	50	DU	0.977	0.975	0.771	0.771
	95	TDDS	0.914	0.914	1.000	1.000
ImageNet	50	DU	0.766	0.779	0.771	0.771
Synthetic CIFAR	95	DU	0.995	0.944	0.943	0.943
		TDDS	0.901	0.940	1.000	1.000

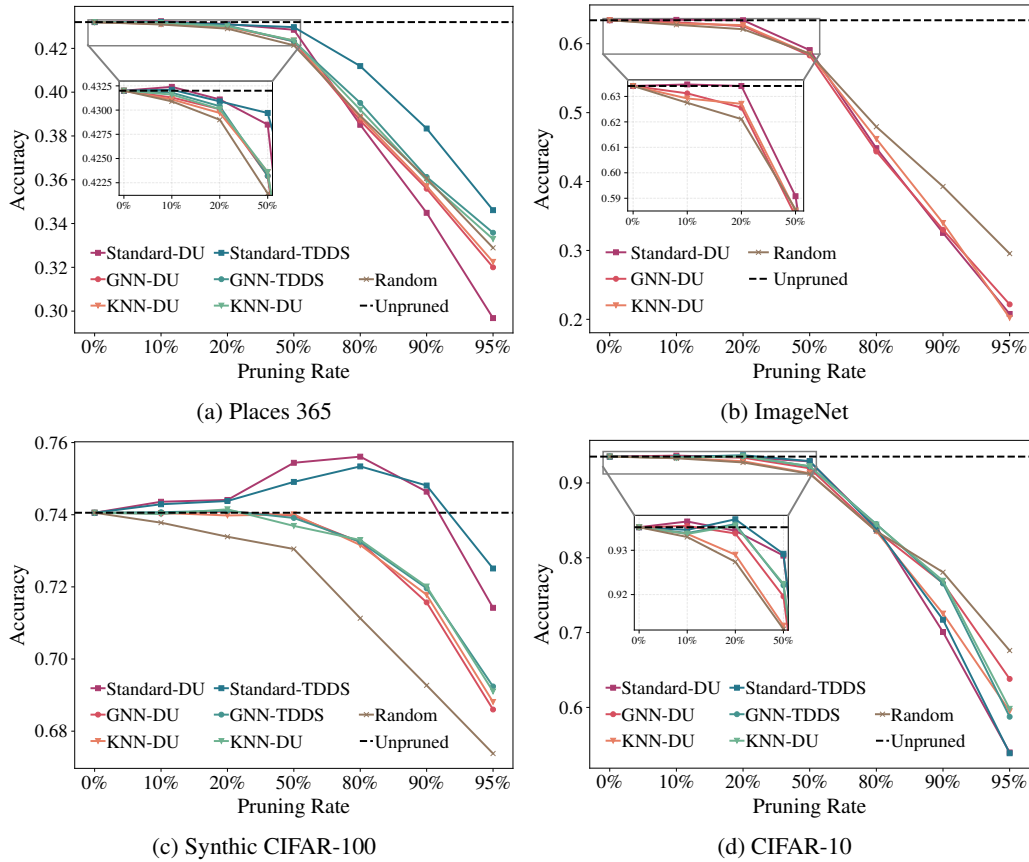


Figure 6: Pruning performance of Standard approaches and their extrapolated counterparts, which started with score computation on 10% subset (20% for CIFAR-10), and then extrapolated with KNN, and GNN.

References

- [1] Shervin Minaee, Tomas Mikolov, Narjes Nikzad, Meysam Chenaghlu, Richard Socher, Xavier Amatriain, and Jianfeng Gao. Large language models: A survey. *Arxiv*, 2402.06196, 2 2024.
- [2] Alexander Kirillov, Eric Mintun, Nikhila Ravi, Hanzi Mao, Chloe Rolland, Laura Gustafson, Tete Xiao, Spencer Whitehead, Alexander C Berg, Wan-Yen Lo, Piotr Dollár, and Ross Girshick. Segment anything. In *Proceedings of the IEEE/CVF International Conference on Computer Vision (ICCV)*, 2023.
- [3] Leon Götze, Marcel Kollovich, Stephan Günnemann, and Leo Schwinn. Efficient time series processing for transformers and state-space models through token merging. In *Proceedings of the International Conference on Machine Learning (ICML)*, 2025.
- [4] Leon Götze, Marcel Kollovich, Stephan Günnemann, and Leo Schwinn. Byte pair encoding for efficient time series forecasting. *arXiv preprint arXiv:2505.14411*, 2025.
- [5] Sebastian Schmidt, Qing Rao, Julian Tatsch, and Alois Knoll. Advanced active learning strategies for object detection. In *Proceedings of the IEEE Intelligent Vehicles Symposium (IV)*, 2020.
- [6] Sebastian Schmidt, Lukas Stappen, Leo Schwinn, and Stephan Günnemann. Generalized synchronized active learning for multi-agent-based data selection on mobile robotic systems. *IEEE Robotics and Automation Letters*, 2024.
- [7] Muyang He, Shuo Yang, Tiejun Huang, and Bo Zhao. Large-scale dataset pruning with dynamic uncertainty. In *Proceedings of the IEEE/CVF Conference on Computer Vision and Pattern Recognition (CVPR)*, 2024.
- [8] Xin Zhang, Jiawei Du, Yunsong Li, Weiyang Xie, and Joey Tianyi Zhou. Spanning training progress: Temporal dual-depth scoring (tdds) for enhanced dataset pruning. In *Proceedings of the IEEE/CVF Conference on Computer Vision and Pattern Recognition (CVPR)*, 2024.
- [9] Andrew Ilyas, Sung Min Park, Logan Engstrom, Guillaume Leclerc, and Aleksander Madry. Datamodels: Predicting predictions from training data. In *Proceedings of the International Conference on Machine Learning (ICML)*. PMLR, 2022.
- [10] Pang Wei Koh and Percy Liang. Understanding black-box predictions via influence functions. In *International conference on machine learning (ICML)*, pages 1885–1894. PMLR, 2017.
- [11] Alex Krizhevsky, Vinod Nair, and Geoffrey Hinton. Learning multiple layers of features from tiny images. Technical report, Canadian Institute for Advanced Research, 2009. URL <http://www.cs.toronto.edu/~kriz/cifar.html>.
- [12] Bolei Zhou, Agata Lapedriza, Aditya Khosla, Aude Oliva, and Antonio Torralba. Places: A 10 million image database for scene recognition. *IEEE Transactions on Pattern Analysis and Machine Intelligence*, 2017.
- [13] Jia Deng, Wei Dong, Richard Socher, Li-Jia Li, Kai Li, and Li Fei-Fei. Imagenet: A large-scale hierarchical image database. In *Proceedings of the IEEE/CVF Conference on Computer Vision and Pattern Recognition (CVPR)*, 2009.
- [14] Ben Sorscher, Robert Geirhos, Shashank Shekhar, Surya Ganguli, and Ari Morcos. Beyond neural scaling laws: beating power law scaling via data pruning. *Advances in Neural Information Processing Systems (NeurIPS)*, 2022.
- [15] Xin Zhang, Jiawei Du, Yunsong Li, Weiyang Xie, and Joey Tianyi Zhou. Spanning training progress: Temporal dual-depth scoring (tdds) for enhanced dataset pruning. In *Proceedings of the IEEE/CVF Conference on Computer Vision and Pattern Recognition (CVPR)*, 2024.
- [16] Ozan Sener and Silvio Savarese. Active learning for convolutional neural networks: A core-set approach. In *International Conference on Learning Representations (ICLR)*, 2018.

- [17] Vitaly Feldman and Chiyuan Zhang. What neural networks memorize and why: Discovering the long tail via influence estimation. *Advances in Neural Information Processing Systems (NeurIPS)*, 33:2881–2891, 2020.
- [18] Chengcheng Guo, Bo Zhao, and Yanbing Bai. Deepcore: A comprehensive library for coreset selection in deep learning. *Database and Expert Systems Applications (DEXA)*, 4 2022.
- [19] Nicholas Gao and Stephan Günnemann. Generalizing neural wave functions. In *International Conference on Machine Learning*, pages 10708–10726. PMLR, 2023.
- [20] Nicholas Gao and Stephan Günnemann. Neural pfaffians: Solving many many-electron schrödinger equations. In *The Thirty-eighth Annual Conference on Neural Information Processing Systems (NeurIPS)*, 2024.
- [21] Björn Nieth, Thomas Altschidl, Leo Schwinn, and Björn Eskofier. Large-scale dataset pruning in adversarial training through data importance extrapolation. In *ICML, DML Workshop*, 2024.
- [22] Haoru Tan, Sitong Wu, Fei Du, Yukang Chen, Zhibin Wang, Fan Wang, and Xiaojuan Qi. Data pruning via moving-one-sample-out. *Advances in neural information processing systems (NeurIPS)*, 2023.
- [23] Mariya Toneva, Alessandro Sordani, Remi Tachet des Combes, Adam Trischler, Yoshua Bengio, and Geoffrey J Gordon. An empirical study of example forgetting during deep neural network learning. In *International Conference on Learning Representations (ICLR)*, 2019.
- [24] Mansheej Paul, Surya Ganguli, and Gintare Karolina Dziugaite. Deep learning on a data diet: Finding important examples early in training. *Advances in Neural Information Processing Systems (NeurIPS)*, 34, 2021.
- [25] Cody Coleman, Christopher Yeh, Stephen Mussmann, Baharan Mirzasoleiman, Peter Bailis, Percy Liang, Jure Leskovec, and Matei Zaharia. Selection via proxy: Efficient data selection for deep learning. In *International Conference on Learning Representations (ICLR)*, 2020.
- [26] Geoff Pleiss, Tianyi Zhang, Ethan Elenberg, and Kilian Q Weinberger. Identifying mislabeled data using the area under the margin ranking. *Advances in Neural Information Processing Systems*, 33:17044–17056, 2020.
- [27] Shuo Yang, Zeke Xie, Hanyu Peng, Min Xu, Mingming Sun, and Ping Li. Dataset pruning: Reducing training data by examining generalization influence. In *International Conference on Learning Representations (ICLR)*, 2023.
- [28] Max Welling and Donald Bren. Herding dynamical weights to learn. In *Proceedings of the International Conference on Machine Learning (ICML)*, 2009.
- [29] Yutian Chen, Max Welling, and Alex Smola. Super-samples from kernel herding. In *Proceedings of the Twenty-Sixth Conference on Uncertainty in Artificial Intelligence (UAI)*, 2010.
- [30] Xiaobo Xia, Jiale Liu, Jun Yu, Xu Shen, Bo Han, and Tongliang Liu. Moderate coreset: A universal method of data selection for real-world data-efficient deep learning. In *the International Conference on Learning Representations (ICLR)*, 2022.
- [31] Xijie Huang, Zechun Liu, Shih-Yang Liu, and Kwang-Ting Cheng. Efficient and robust quantization-aware training via adaptive coreset selection. *Transaction on Machine Learning (TMLR)*, 8 2024.
- [32] Baharan Mirzasoleiman, Jeff Bilmes, and Jure Leskovec. Coresets for data-efficient training of machine learning models. In *Proceedings of the International Conference on Machine Learning (ICML)*, 2020.
- [33] Sarel Har-Peled, Dan Roth, and Dav A Zimak. Maximum margin coresets for active and noise tolerant learning. In *Proceedings of the international joint conference on Artificial intelligence (JCAI)*, 2006.
- [34] Haizhong Zheng, Rui Liu, Fan Lai, and Atul Prakash. Coverage-centric coreset selection for high pruning rates. In *International Conference on Learning Representations (ICLR)*, 2023.

- [35] Brent A Griffin, Jacob Marks, and Jason J Corso. Zero-shot coreset selection: Efficient pruning for unlabeled data. *Arxiv*, 2411.15349, 2024.
- [36] Zalán Borsos, Mojmir Mutny, and Andreas Krause. Coresets via bilevel optimization for continual learning and streaming. In *Advances in Neural Information Processing Systems (NeurIPS)*, volume 33, pages 14879–14890, 2020.
- [37] Krishnateja Killamsetty, Durga Sivasubramanian, Ganesh Ramakrishnan, and Rishabh Iyer. Glister: Generalization based data subset selection for efficient and robust learning. In *Proceedings of the AAAI Conference on Artificial Intelligence*, volume 35, 2021.
- [38] Krishnateja Killamsetty, Sivasubramanian Durga, Ganesh Ramakrishnan, Abir De, and Rishabh Iyer. Grad-match: Gradient matching based data subset selection for efficient deep model training. In *International Conference on Machine Learning*, pages 5464–5474. PMLR, 2021.
- [39] Aleksander Madry, Aleksandar Makelov, Ludwig Schmidt, Dimitris Tsipras, and Adrian Vladu. Towards deep learning models resistant to adversarial attacks. *arXiv preprint arXiv:1706.06083*, 2017.
- [40] Leon Bungert, René Raab, Tim Roith, Leo Schwinn, and Daniel Tenbrinck. Clip: Cheap lipschitz training of neural networks. In *International Conference on Scale Space and Variational Methods in Computer Vision*, pages 307–319. Springer International Publishing Cham, 2021.
- [41] Zekai Wang, Tianyu Pang, Chao Du, Min Lin, Weiwei Liu, and Shuicheng Yan. Better diffusion models further improve adversarial training. In *International Conference on Machine Learning (ICML)*, 2023.
- [42] Thomas Altstidl, David Dobre, Björn Eskofier, Gauthier Gidel, and Leo Schwinn. On the scalability of certified adversarial robustness with generated data. In *NeurIPS*, 2024.
- [43] Sophie Xhonneux, Alessandro Sordoni, Stephan Günnemann, Gauthier Gidel, and Leo Schwinn. Efficient adversarial training in llms with continuous attacks. In *NeurIPS*, 2024.
- [44] Leo Schwinn, An Nguyen, René Raab, Leon Bungert, Daniel Tenbrinck, Dario Zanca, Martin Burger, and Bjoern Eskofier. Identifying untrustworthy predictions in neural networks by geometric gradient analysis. In *UAI*, pages 854–864. PMLR, 2021.
- [45] Leo Schwinn, Leon Bungert, An Nguyen, René Raab, Falk Pulsmeier, Doina Precup, Björn Eskofier, and Dario Zanca. Improving robustness against real-world and worst-case distribution shifts through decision region quantification. In *Proceedings of the International Conference on Machine Learning (ICML)*, pages 19434–19449, 2022.
- [46] Jan Schuchardt, Johannes Gasteiger, Aleksandar Bojchevski, and Stephan Günnemann. Collective robustness certificates: Exploiting interdependence in graph neural networks. In *International Conference on Learning Representations*, 2021.
- [47] Jan Schuchardt and Stephan Günnemann. Invariance-aware randomized smoothing certificates. In *Conference on Neural Information Processing Systems (NeurIPS)*, 2022.
- [48] Leo Schwinn, An Nguyen, René Raab, Dario Zanca, Bjoern M Eskofier, Daniel Tenbrinck, and Martin Burger. Dynamically sampled nonlocal gradients for stronger adversarial attacks. In *2021 International Joint Conference on Neural Networks (IJCNN)*, pages 1–8. IEEE, 2021.
- [49] Leo Schwinn, René Raab, An Nguyen, Dario Zanca, and Bjoern Eskofier. Exploring misclassifications of robust neural networks to enhance adversarial attacks. *Applied Intelligence*, 2023.
- [50] Marcel Kolloviah, Lukas Gosch, Yan Scholten, Marten Lienen, Leo Schwinn, and Stephan Günnemann. Assessing robustness via score-based adversarial image generation. *Transactions on Machine Learning Research (TMLR)*, 2023.
- [51] Jan Schuchardt, Tom Wollschläger, Aleksandar Bojchevski, and Stephan Günnemann. Localized randomized smoothing for collective robustness certification. In *International Conference on Learning Representations (ICLR)*, 2023.

- [52] Weizhe Hua, Yichi Zhang, Chuan Guo, Zhiru Zhang, and G. Edward Suh. BulletTrain: Accelerating robust neural network training via boundary example mining. In *Advances in Neural Information Processing Systems (NeurIPS)*, 2021.
- [53] Erh-Chung Chen and Che-Rung Lee. Data filtering for efficient adversarial training. *Pattern Recognition*, 151, 2024.
- [54] Krishnateja Killamsetty, Durga Sivasubramanian, Ganesh Ramakrishnan, Abir De, and Rishabh Iyer. GRAD-MATCH: Gradient matching based data subset selection for efficient deep model training. *PMLR*, 2021.
- [55] Hadi M. Dolatabadi, Sarah Erfani, and Christopher Leckie. Adversarial coreset selection for efficient robust training. *International Journal of Computer Vision*, 131(12):3307–3331, 2023.
- [56] Maximilian Kaufmann, Yiren Zhao, Ilia Shumailov, Robert Mullins, and Nicolas Papernot. Efficient adversarial training with data pruning. *Arxiv*, 2207.00694, 2022.
- [57] Yize Li, Pu Zhao, Xue Lin, Bhavya Kailkhura, and Ryan Goldhahn. Less is more: Data pruning for faster adversarial training. *Arxiv*, 2302.12366, 2023.
- [58] Liyuan Wang, Xingxing Zhang, Hang Su, and Jun Zhu. A comprehensive survey of continual learning: Theory, method and application. *IEEE Transactions on Pattern Analysis and Machine Intelligence*, 46, 8 2024.
- [59] Tongzhou Wang, Jun-Yan Zhu, Antonio Torralba, and Alexei A. Efros. Dataset distillation. *Arxiv*, 1811.10959, 11 2018.
- [60] Christopher J. Holder and Muhammad Shafique. Efficient uncertainty estimation in semantic segmentation via distillation. In *Proceedings of the IEEE/CVF International Conference on Computer Vision (ICCV)*, 2021.
- [61] Andreas Kirsch and Yarin Gal. Unifying approaches in active learning and active sampling via fisher information and information-theoretic quantities. *Transactions on Machine Learning Research (TMLR)*, 2022.
- [62] Sebastian Schmidt, Leonard Schenk, Leo Schwinn, and Stephan Günnemann. A unified approach towards active learning and out-of-distribution detection. *arXiv preprint arXiv:2405.11337*, 2024.
- [63] Sebastian Schmidt, Leonard Schenk, Leo Schwinn, and Stephan Günnemann. Joint out-of-distribution filtering and data discovery active learning. In *Proceedings of the IEEE/CVF Conference on Computer Vision and Pattern Recognition (CVPR)*, 2025.
- [64] Christoffer Löffler and Christopher Mutschler. Iale: Imitating active learner ensembles. *Journal of Machine Learning Research*, 23(107):1–29, 2022.
- [65] Christoffer Löffler, Kion Fallah, Stefano Fenu, Dario Zanca, Bjoern Eskofier, Christopher John Rozell, and Christopher Mutschler. Active learning of ordinal embeddings: A user study on football data. *Transactions on Machine Learning Research*, 2023.
- [66] Patrik Okanovic, Roger Waleffe, Vasilis Mageirakos, Konstantinos E. Nikolakakis, Amin Karbasi, Dionysis Kalogierias, Nezihe Merve Gürel, and Theodoros Rekatsinas. Repeated random sampling for minimizing the time-to-accuracy of learning. In *Proceedings of the International Conference on Learning Representations (ICLR)*, 5 2024.
- [67] Zhenyu Tang, Shaoting Zhang, and Xiaosong Wang. Exploring data redundancy in real-world image classification through data selection. *Arxiv*, 2306.14113, 2023.
- [68] Thomas N Kipf and Max Welling. Semi-supervised classification with graph convolutional networks. In *International Conference on Learning Representations (ICLR)*, 2017.
- [69] Will Hamilton, Zhitao Ying, and Jure Leskovec. Inductive representation learning on large graphs. *Advances in Neural Information Processing Systems (NeurIPS)*, 30, 2017.

- [70] Jacob Benesty, Jingdong Chen, Yiteng Huang, and Israel Cohen. Pearson correlation coefficient. In *Noise reduction in speech processing*, pages 37–40. Springer, 2009.
- [71] Jerrold H Zar. Spearman rank correlation. *Encyclopedia of Biostatistics*, 7, 2005.
- [72] Artyom Gadetsky, Yulun Jiang, and Maria Brbic. Let go of your labels with unsupervised transfer. In *Proceedings of the International Conference on Machine Learning (ICML)*. PMLR, 6 2024.
- [73] Jonathan Ho, Ajay Jain, and Pieter Abbeel. Denoising diffusion probabilistic models. *Advances in Neural Information Processing Systems (NeurIPS)*, 33:6840–6851, 2020.
- [74] Kaiming He, Xiangyu Zhang, Shaoqing Ren, and Jian Sun. Deep residual learning for image recognition. In *Proceedings of the IEEE/CVF Conference on Computer Vision and Pattern Recognition (CVPR)*, pages 770–778, 2016.
- [75] Sergey Zagoruyko and Nikos Komodakis. Wide residual networks. In *Proceedings of the British Machine Vision Conference (BMVC)*, 2016.
- [76] Maxime Oquab, Timothée Darcet, Théo Moutakanni, Huy Vo, Marc Szafraniec, Vasil Khalidov, Pierre Fernandez, Daniel Haziza, Francisco Massa, Alaaeldin El-Nouby, et al. Dinov2: Learning robust visual features without supervision. *arXiv preprint arXiv:2304.07193*, 2023.
- [77] Diederik P Kingma and Jimmy Ba. Adam: A method for stochastic optimization. In *International Conference on Learning Representations (ICLR)*, 2015.
- [78] Ilya Sutskever, James Martens, George Dahl, and Geoffrey Hinton. On the importance of initialization and momentum in deep learning. In *International Conference on Machine Learning (ICML)*, pages 1139–1147. PMLR, 2013.
- [79] Ilya Loshchilov and Frank Hutter. Sgdr: Stochastic gradient descent with warm restarts. In *International Conference on Learning Representations (ICLR)*, 2017.
- [80] Leslie N Smith and Nicholay Topin. Super-convergence: Very fast training of neural networks using large learning rates. In *Artificial intelligence and machine learning for multi-domain operations applications*, volume 11006, pages 369–386. SPIE, 2019.